The flanking peptides issue from the maturation of the human islet amyloid polypeptide (hIAPP) slightly modulate hIAPP-fibril formation but not hIAPP-induced cell death

Shadai Salazar Vazquez, Bertrand Blondeau, Pierre Cattan, Mathieu Armanet, Ghislaine Guillemain, Lucie Khemtemourian

The flanking peptides issue from the maturation of the human islet amyloid polypeptide (hIAPP) slightly modulate hIAPP-fibril formation but not hIAPP-induced cell death.

Shadai Salazar Vazquez[1], Bertrand Blondeau[2], Pierre Cattan[3], Mathieu Armanet[3], Ghislaine Guillemain[2,*], Lucie Khemtemourian[1,*]

[1] Sorbonne Université, Ecole Normale Supérieure, PSL University, CNRS, Laboratoire des Biomolécules (LBM), 4 place Jussieu, F-75005 Paris, France

[2] Sorbonne Université, Inserm UMR_S938, Centre de recherche de St-Antoine, Lipodystrophies, adaptations métaboliques et hormonales, et vieillissement, 27 rue de Chaligny, 75012 Paris, France

[3] Cell Therapy Unit, Hospital Saint-Louis and University Paris-Diderot, Paris, France.

[*]To whom correspondence should be addressed: Tel: +33 1 44 27 61 83; +33 1 40 01 13 54; E-mail address: lucie.khemtemourian@upmc.fr; ghislaine.guillemain@inserm.fr

GG and LK contributed equally to the publication.

Abbreviations

hIAPP, human Islet Amyloid Polypeptide; CD, circular dichroism; LUVs, large unilamellar vesicles; T2DM, type 2 diabetes mellitus; TEM, transmission electron microscopy; TFA, trifluoroacetic acid; ThT, Thioflavin T.

Abstract

Type 2 diabetes mellitus is a disease characterized by the formation of amyloid fibrillar deposits consisting mainly in human islet amyloid polypeptide (hIAPP), a peptide co-produced and co-secreted with insulin. hIAPP and insulin are synthesized by pancreatic β cells initially as prehormones resulting after sequential cleavages in the mature peptides as well as the two flanking peptides (N- and C-terminal) and the C-peptide, respectively. It has been suggested that in the secretory granules, the kinetics of hIAPP fibril formation could be modulated by some internal factors. Indeed, insulin is known to be a potent inhibitor of hIAPP fibril formation and hIAPP-induced cell toxicity. Here we investigate whether the flanking peptides could regulate hIAPP fibril formation and toxicity by combining biophysical and biological approaches. Our data reveal that both flanking peptides are not amyloidogenic. In solution and in the presence of phospholipid membranes, they are not able to totally inhibit hIAPP-fibril formation neither hIAPP-membrane damage. In the presence of INS-1 cells, a rat pancreatic β-cell line, the flanking peptides do not modulate hIAPP fibrillation neither hIAPP-induced cell death while in the presence of human islets, they have a slightly tendency to reduce hIAPP fibril formation but not its toxicity. These data demonstrate that the flanking peptides do not strongly contribute to reduce mature hIAPP amyloidogenesis in solution and in living cells, suggesting that other biochemical factors present in the cells must act on mature hIAPP fibril formation and hIAPP-induced cell death.

Keywords: islet amyloid polypeptide; amyloid fibril formation; maturation peptides; cell and islet toxicity; type 2 diabetes mellitus;

1. Introduction

Protein misfolding and aggregation that lead to insoluble fibrils are the key factors for several human diseases, such as type 2 diabetes mellitus (T2DM), Alzheimer's disease, Parkinson's disease, Prion diseases as well as for many physiological processes [1,2]. In most of these misfolded protein diseases, the natively unfolded protein converts into insoluble ordered fibrillary aggregates, called as amyloid fibrils. The aggregation of amyloid proteins is a well-known process that leads to the formation of fibrils at the surface of cells, associated with cell toxicity [2–4]. In T2DM, the amyloid fibrils are found in the pancreatic islets of patients and are mainly composed of the human islet amyloid polypeptide (hIAPP), a 37 amino acid peptide (also known as amylin) [5,6].

hIAPP is coproduced and co-secreted along with insulin through the secretory pathway in a molar hIAPP:insulin ratio of 1:100 in healthy individuals, a ratio that can increase to 1:20 in T2DM [7,8]. During protein translation, hIAPP is processed and modified. Both hIAPP and insulin are secretory proteins initially synthesized as preprohormones that are released in response to stimuli [9–11]. Both hIAPP and insulin possess signal peptides that drive the targeting of nascent polypeptides from the cytosol to the endoplasmic reticulum (ER), the entry point into the secretory pathway [12,13]. The N-terminal signal peptides are removed by signal peptidase resulting in prohIAPP and proinsulin. In the oxidizing environment of the ER lumen, prohIAPP and proinsulin rapidly fold to form respectively one and three disulfide bonds, all evolutionary conserved. The resulting 67 amino acids prohIAPP and 86 amino acids proinsulin are cleaved in the *trans*-golgi network and then in the secretory granules by the prohormone convertases (PC1/3 and PC2) in concert with carboxypeptidase E (CPE) leading to the mature hIAPP and mature insulin. C-peptide resulting from proinsulin maturation as well

as the two flanking peptides resulting from prohIAPP processing remain in the secretory granules.

The composition of the β-cell granule is extremely complex and contains many components that could influence hIAPP fibril formation and hIAPP toxicity. In fact, it is still not understood why and how hIAPP forms amyloid fibrils. However, several studies demonstrated that aggregation of amyloid proteins is easily influenced by both intrinsic features, such as mutations, expression levels, presence of peptides from the maturation, and by extrinsic factors, such as macromolecular crowding and interaction with metal ions, lipid membranes, or chaperones [14–26]. In the case of hIAPP, it was shown that divalent metal ion, Zn(II) and Cu(II) slowed down the kinetics of fibril formation, probably through the histidine residue at position 18 as a site of interaction and/or by forming a stable non fibrillar hIAPP-metal complex [17, 27-29]. However, the role of Cu(II) in hIAPP-induced cell death has been controversial. A few studies demonstrated that hIAPP-induced INS-1 cells toxicity increased in the presence of Cu(II) [28, 30-31] while another study on INS-1 cells and also on SHSY5Y cells, reported that copper ions do not affect hIAPP-induced cell death [29]. In addition to metal ions, granule peptides such as insulin and the C-peptide could also modify hIAPP fibril formation and hIAPP-induced cell death. Westermark *et al.* demonstrated first that insulin, even at a low concentration, significantly inhibited hIAPP fibril formation [32]. Later, several studies confirmed this statement and proposed different mechanism of an inhibition process [33-35]. Importantly, C-peptide, which do not form fibril itself, could reduce the amount of hIAPP fibrils [32]. It was shown that lowering pH to mimic the acid environment of the granules protects hIAPP from fibril formation *in vitro* [16] and that the histidine residue 18, the only residue that titrates over the pH range, plays an important role in hIAPP aggregation and misfolding [36]. Finally, a study revealed that the prohIAPP prevents aggregation and

membrane damage of mature hIAPP [37]. However, no data are currently available on a putative function of both flanking peptides neither on their influence on hIAPP fibril formation and on hIAPP toxicity. Our goal was to determine if hIAPP flanking peptides could present some physiological properties and more specifically could form fibrils and/or affect hIAPP fibrillation and toxicity. This question about a functional role of hIAPP flanking peptide was asked, as the C-peptide, which comes from the insulin maturation process, has been described as an active molecule. Indeed, for a long time, it has been thought that the C-peptide has no physiological effect and it was used as a biomarker of pancreatic β-cell activity. Since the last 20 years, the interest upon a biological action of C-peptide has grown. So far, the physiological effect of C-peptide remains unknown. In contrast, in type 1 diabetic patients, a positive effect on microvascular complications of diabetes has been demonstrated. More specifically, the C-peptide plays a neuro- and a reno-protective effects, stimulates the pancreatic β-cell antioxidant capacity and could present an anti-inflammatory action [38]. It has also been proposed that the C-peptide could promote insulin release from it aggregated storage form, enhancing the insulin biological effect [39].

To shed light on hIAPP flanking peptides function, a comprehensive set of both biophysical experiments (fluorescence, circular dichroism, transmission electron microscopy) and biological studies were performed in solution, in the presence of membrane models, on culture cells and on human pancreatic islets. In particular, we investigated the ability of the flanking peptides to form fibrils, their secondary structures, their effect on mature hIAPP fibril formation and their influence on cell toxicity. We found in solution and in the presence of model membranes that the flanking peptides are not able to completely inhibit hIAPP fibril formation and hIAPP-induced membrane leakage. In the presence of INS-1 cells, the flanking peptides appear to have no effect on the hIAPP fibril formation neither on cell toxicity.

However, in human pancreatic islets both flanking peptides slightly reduce hIAPP fibril formation but not hIAPP toxicity.

2. Materials and Methods

2.1. Materials

1,2-dioleoyl-sn-glycero-3-phosphocholine (DOPC) and 1,2-dioleoyl-sn-glycero-3-phospho-L-serine (DOPS) were obtained from Avanti Polar Lipids (Alabaster, USA). Thioflavin T (ThT) and calcein were obtained from Sigma-Aldrich (Saint Quentin Fallavier, France). Cell culture media were obtained from ThermoFisher scientific (France).

2.2. Peptide synthesis and preparation

Mature hIAPP and the two flanking peptides were synthesized with a CEM Liberty Blue (CEM corporation, Matthews, USA) automated microwave peptide synthesizer using standard reaction cycles at the Institut de Biologie Intégrative (IFR83 - Sorbonne Université). The synthesis of mature hIAPP with an amidated C-terminus and a disulfide bridge was performed as described [36]. The synthesis of all peptides was performed using Fmoc chemistry and a PAL Novasyn TG resin. For mature hIAPP, two pseudoproline dipeptides were chosen for the synthesis Fmoc-Ala-Thr(ΨMe,MePro)-OH replaced residues Ala-8 and Thr-9, and Fmoc-Leu-Ser(ΨMe,MePro)-OH replaced residues Leu-27 and Ser-28. Double couplings were performed for the pseudoprolines and for the residues following the pseudoprolines and for every β-branched residue. The three peptides were cleaved from the resin and deprotected using standard TFA procedures with 1,2-ethanedithiol, water, and trisiopropylsilane as scavengers. The three peptides were purified by reverse phase high-performance liquid chromatography (HPLC) with a Luna C18(2) column (Phenomenex, USA). A two-buffer system was used. Buffer A consisted of 100% H2O and 0.1% TFA (vol/vol), and buffer B consisted of 100% acetonitrile

and 0.07% TFA (vol/vol). Mature linear hIAPP was dissolved in aqueous DMSO (33%) and oxidized with air to the corresponding disulfide bond. Purity of peptides was higher than 95% as determined by analytical HPLC and identity of peptides was confirmed by MALDI-TOF mass spectrometry.

An essential criterion for measuring aggregation kinetics of amyloid peptides is to start with a monomeric form of the peptide. Therefore, peptide stock solutions were freshly prepared prior to all experiments using the same batch. Peptide stock solutions were prepared as described previously [36]. Briefly, stock solutions were obtained by dissolving the peptide at a concentration of 1 mM in hexafluoroisopropanol (HFIP) followed by one hour incubation. Then, HFIP was evaporated and the sample was dried by vacuum desiccation for at least 30 min. The resulting peptide film was dissolved at a concentration of 1 mM in DMSO for the fluorescence experiments (final DMSO concentration of 2.5% v/v) and then diluted in 20 mM Tris-HCl, 100 mM NaCl at pH 7.4. Both DMSO and NaCl interfere with the circular dichroism experiments, therefore in these experiments the peptide film was directly dissolved in a 20 mM sodium phosphate buffer, 100 mM NaF at pH 7.4. For the biological assay the peptide film was directly dissolved in the culture media.

2.3. Determination of peptide aggregation by thioflavin-T assay

The kinetics of fibril formation was measured using the fluorescence intensity increase upon binding of the fluorescent probes Thioflavin T (ThT) to fibrils. A plate reader (Fluostar Optima, BMG LabTech, Germany) and a standard 96 wells black microtiter plate were used. The fluorescence was measured at room temperature every 10 minutes (excitation filter λ =440 nm and emission filter λ=480 nm).

The fluorescence assay in solution was started by adding 10 µL of a 0.2 mM hIAPP in DMSO to 190 µl of a mixture of 10 µM ThT and 20 mM Tris-HCl, 100 mM NaCl at pH 7.4. The ThT

fluorescence assay in the presence of membrane models was started by adding 10 µL of a 0.2 mM IAPP (10 µM peptide) to 190 µL of a mixture of 10 µM ThT, DOPC/DOPS vesicles (100 µM lipids; peptide:lipid ratio 1:10) and 20 mM Tris-HCl, 100 mM NaCl at pH 7.4. For the hIAPP:flanking peptides experiments, the ThT assay was started by adding 10 µL of a 0.2 mM hIAPP and 10 µL of a 0.2 mM flanking peptides to 180 µL of a mixture of 10 µM ThT and 20 mM Tris-HCl, 100 mM NaCl at pH 7.4. The microtiter plate was shaken for 10 seconds (600 rpm) directly after addition of all components, but not during the measurements. The assays were performed 3 times, each in triplicate, on different days, using different peptides stock solutions. The replicates of each system showed consistent reproducibility.

The resulting curves were analyzed using Origin® program and fitted to a Boltzman sigmoidal equation, where F_i and F_t are the initial and final fluorescence values. This fitting allows the estimation of kinetic parameters such as the time for which the fluorescence reaches 50% of its maximal intensity ($t_{1/2}$).

$$F = \frac{Fi - Ff}{1 + e^{(t - t1/2)/\tau}} + Ff$$

2.4. Transmission Electron Microscopy (TEM)

TEM was performed at the "Institut de Biologie Paris Seine" (IBPS, Sorbonne Université, Paris, France). Aliquots (20 µL) of the samples used for fluorescence assays were removed at the end of each kinetic experiments, blotted on a glow-discharged carbon coated 200 mesh copper grids for 2 minutes and then negatively stained with saturated uranyl acetate for 45 seconds. Grids were examined using a JEOL electron microscope operating at 80 kV.

2.5. Circular dichroism

The secondary structure of peptides was measured using a Jasco J-815 CD spectropolarimeter with a Peltier temperature-controlled cell holder over the wavelength range 190-260 nm.

Measurements were carried out in cells of 0.1 cm path length at 25°C in 20 mM phosphate buffer, 100 mM NaF at pH 7.4. Measurements were taken every 0.2 nm at a scan rate of 10 nm/min. Four scans were accumulated and averaged. Peptide concentration was 25 µM. The background spectrum was subtracted and the results were expressed as molar ellipiticity per residue (degree.dmol^{-1}.cm^2.residue^{-1}), and are given by:

$$[\theta_{molar}] = \frac{100 \times \theta}{c \times l \times N}$$

where θ is the recorded ellipticity in degrees, c is the peptide concentration in dmol.L^{-1}, l is the cell path-length in cm and N is the number of peptidic bound.

2.6. Membranes preparation

The vesicles were composed of a mixture of DOPC/DOPS in a 7:3 molar ratio. Stock solutions of DOPC and DOPS in chloroform at concentrations of 20-30 mM were mixed in a glass tube. The solvent was evaporated with dry nitrogen gas yielding a lipid film that was subsequently kept in a vacuum desiccator for 20 min. Lipid films were then rehydrated with 20 mM Tris-HCl, 100 mM NaCl at pH 7.4 at a temperature above the transition temperature of the lipids for 30 min. The lipid suspensions were subjected to 10 freezethaw cycles, at temperatures of approximately 80 and 40 °C, respectively, and subsequently extruded 19 times through a mini-extruder (Avanti Polar Lipids, Alabaster, USA) equipped with a 200 nm polycarbonate membrane. The phospholipid content of lipid stock solutions and vesicle preparations was determined as inorganic phosphate according to Rouser [40]. Calcein-containing large unilamellar vesicles (LUVs) were made using the same protocol, except for the following adaptations. The buffer for hydration of the lipid films was replaced by a solution containing 70 mM calcein in 50 mM Tris-HCl. Free calcein was separated from the calcein-filled LUVs using

size-exclusion chromatography (Sephadex G50-fine) and elution with 20 mM Tris-HCl, 100 mM NaCl (pH 7.4).

2.7. Vesicle Dye Leakage Assay

A plate reader (Fluostar Optima, Bmg Labtech) was used to perform calcein leakage experiments in standard 96-well transparent microtiter plates. Measurements were conducted on calcein-loaded DOPC/DOPS 7:3. hIAPP in the absence or in the presence of a flanking peptides was added to a mixture of calcein-containing LUVs in 20 mM Tris-HCl, 100 mM NaCl, pH 7.4 buffer. The final concentrations were 100 µM for lipids and 10 µM for peptide (peptide:lipid ratio of 1:10). Directly after addition of all components, the microtiter plate was shaken for 10 s using the shaking function of the plate reader. The plate was not shaken during the measurement. Fluorescence was measured from the bottom, every minute, using a 485 nm excitation filter and a 520 nm emission filter. The temperature was approximately 28 °C ± 3 °C. The maximum leakage at the end of each measurement was determined via addition of 2 µL of 10% Triton-X100 to a final concentration of 0.05% (v/v). The release of fluorescent dye was normalized according to the following equation:

$$L_T = \frac{F_T - F_0}{F_{100} - F_0}$$

In this equation, L_T is the fraction of dye released (normalized membrane leakage), F_T is the measured fluorescence intensity, and F_0 and F_{100} are the fluorescence intensities at time zero and after addition of Triton-X100, respectively. The calcein leakage experiment was performed 3 times, each in triplicate, on different days. The results presented here are the average of the different experiments ± standard deviation.

2.8. Cell culture

Rat insulinoma-1 (INS-1) pancreatic β-cells were grown in culture medium containing RPMI 1640 supplemented with penicillin (100 units/ml), streptomycin (100 µg/ml), β -mercapto-ethanol (50 µM), pyruvate (1 µM) and 10% heat-inactivated calf serum. The cultures were maintained at 37 °C in humidified 95% air, 5% CO_2.

2.9. Human islet culture

Human islets batches were provided by the Cell Therapy Unit (Saint-Louis Hospital, Paris). Human islets were cultured in RPMI 1640 supplemented with penicillin (100 units/ml), streptomycin (100 µg/ml), and 10% heat-inactivated calf serum. The cultures were maintained at 37 °C in humidified 95% air, 5% CO_2.

2.10. Fibril formation in presence of cells or islets

INS-1 cells and human islets were plated respectively at a density of 30 000 cells/well or 50 islets/well in a 96-wells black plate. Following 24 hours of incubation, the medium was replaced with 100 µl of fresh medium containing 50 µM of indicated peptide. Two µl (final concentration 20 µM) of Thioflavine T was added in each well in order to monitor fibril formation. The fluorescence was measured at 30°C from the top of the plate every 30 minutes with excitation filter 440 nm and emission filter 485 nm for a 24 h (INS-1 cells) or a 48 h period (human islets). The assays were performed 3 times, each in triplicate, on different cell line cultures, using different peptide stock solutions. All values represent means ± the standard error of the mean (N=3).

2.11. MTT Cell Toxicity Assay

MTT-based cell toxicity assay was used to assess cell metabolic activity [41]. The cell growth is measured as a function of mitochondrial activity in living cells. Low absorbance values indicate a reduction in cell viability. The MTT cell assays were performed according to the

manufacturer's instructions (Sigma Aldrich, France). Briefly, the INS-1 cells and human islets were plated respectively at a density of 30 000 cells/well or 50 islets/well in a 96-wells plate. Following 24 hours of incubation, the medium was replaced with 100 µl of fresh medium containing 50 µM of indicated peptide. Cells were further incubated for 24 h (INS-1 Cells) or 48 h (human islets). Ten µl of MTT solution (5 mg/mL) was added to each well and further incubated for 3 hours. The culture medium was then removed and 100 µL of MTT solvent were added. The well-plate was gently shaken during 30 minutes and the absorbance was measured at 550 nm within 30 min after adding MTT solvent. Values were calculated relative to those of control cells treated with buffer only. The assays were performed 3 times, each in triplicate, on different cell line cultures, using different peptide stock solutions. All values represent means ± the standard error of the mean (N=3).

2.12.Statistics

Each experiment was performed at least 3 times in triplicates. Results are expressed, as means ± SEM. Statistical significance was determined using a one-way ANOVA for MTT experiments and a two-way ANOVA for ThT fibrillation studies.

3. Results

3.1. The flanking peptide are not amyloidogenic in solution

Fig. 1 shows steps of hIAPP maturation and peptides sequences. To predict the amyloidogenicity of the flanking peptides, we first analyzed their amino acids sequences in comparison with that of mature hIAPP using several standard amyloid prediction programs. The first method relies on individual amino acid aggregation propensities and on the composition of amyloidogenic regions. The two most popular programs, AGGRESCAN [42] and FoldAmyloid [43], demonstrate that the N-terminal flanking peptide is not amyloidogenic and

the C-terminal peptide gives contradictory results (not amyloidogenic with AGGRESCAN and amyloidogenic with FoldAmyloid) (Table 1). Then, we used the program TANGO that relies on individual amino acid aggregation propensities and on the properties of β-structural conformation [44]. The result shows that the N-terminal peptide is not amyloidogenic (score 0) while the C-terminal peptide is a little amyloidogenic (score 4.10) compared with mature hIAPP (score 43.78), consistent with the FoldAmyloid program. Finally, we tested two programs, ZipperDB [45] and Waltz[46], based on the analysis of 3D amyloid-like structures of short peptides. These two programs support the previous results for the N-terminal peptides. However they gave inconsistent results for the C-terminal peptide: 2 amyloidogenic segments with ZipperDB and none with Waltz (Table 1). Since the amyloid prediction programs provided unreliable results for the C-terminal flanking peptide, we experimentally evaluated the amyloidogenicity of both flanking peptides.

First, we studied the time course of the aggregation of the flanking peptides and mature hIAPP in solution by using thioflavin-T (ThT) binding fluorescence assays, which is a widely used method to monitor amyloid fibril formation [47]. Fig. 2A shows typical sigmoidal curves obtained for hIAPP at different concentrations (5 to 100 μM). For hIAPP at 5 μM, the transition from monomer to fibril formation occurs after 4.4 h ± 0.5, consistent with previous results [48]. To obtain a clear picture of the molecular mechanisms that give rise to hIAPP fibrils, we analyzed the effect of varying hIAPP initial concentration on $t_{1/2}$ values. The value of the scaling exponent, which describes how the $t_{1/2}$ of the reaction scales with the initial concentration of hIAPP monomer, was measured in Figure 2B. The $t_{1/2}$ demonstrates a concentration dependence as a power function $t_{1/2} \sim c^{\gamma}$, with an exponent γ of -0.14 consistent with previous results [48]. In contrast, at the same range of concentration both flanking peptides do not form fibrils even after 2 days of experiments (Fig. 2C).

The ThT dye provides a convenient assay of amyloid formation kinetics but can lead to false negatives. Thus, we used transmission electron microscopy (TEM) to independently monitor amyloid formation. After incubation for 1 day, mature hIAPP formed fibrils with the typical morphology of amyloid fibrils (Fig. 3A). In contrast, no fibrils could be detected, even after incubation for 4 days with the flanking peptides (Fig. 3B-C), consistent with the ThT experiments.

It has been shown that the conformation of hIAPP in solution changes within a few hours from random col to β-sheet, indicative of amyloid fibrils [49]. We performed CD measurements to analyze the conformational changes of the peptides after a few hours of incubation. The CD spectra of mature hIAPP, at the start of the incubation, displays a peak with negative ellipticity at 200 nm that is characteristic of a random coil conformation. After a few hours of incubation, hIAPP adopts a β-sheet structure, indicated by the appearance of a negative band at 220 nm and the loss of the negative band at 200 nm (Fig. 3D). In contrast, the CD signals of the flanking peptides retain their random coil conformation for at least 48 h, indicative the absence of amyloid fibril formation under these conditions (Fig. 3E-F). Altogether, our data demonstrate that the flanking peptides are not fibrillogenic in solution.

3.2. The C- and N-terminal flanking peptides are not amyloidogenic in artificial vesicles nor in cells

hIAPP aggregation in the presence of model lipidic membranes was and still is an intensely investigated issue [20, 25, 50-52]. Previous results indicated that changes in lipid composition significantly contribute to the disruption of peptides-membranes interactions, peptides misfolding and aggregation [50, 53]. In particular, the presence of negatively charged lipids accelerates the rate of hIAPP fibril formation [20,50], which led us to study the flanking peptides-fibril formation in the presence of anionic lipids. The same fluorescence experiments

were carried out in the presence of large unilamellar vesicles (LUVs) composed of a mixture of the zwitterionic lipid phosphatidylcholine (DOPC) and the anionic lipid phosphatidylserine (PS) in a 7:3 molar ratio to mimic the membranes of pancreatic islet cells [54]. As expected, at a concentration of 10 μM mature hIAPP rapidly formed amyloid fibrils when incubated with theses vesicles with a $t_{1/2}$ of 2.8 h, whereas neither C-terminal peptide nor N-terminal peptide was found to form fibrils (Fig. 4AB). Then the ability of the peptides, mature hIAPP and the two flanking peptides, to permeabilize LUVs was examined by measuring the fluorescence signal of the encapsulated fluorophore, calcein. A time trace of calcein leakage induced by mature hIAPP is shown in Fig.4A (blue). Mature hIAPP induced an extent of membrane leakage of 62 ± 5% consistent with previous results [55]. However, no membrane leakage was observed for both flanking peptides (Fig. 4A).

Many extrinsic factors, such as macromolecular crowding could influence the structure, the fibril formation and the membrane-interactions of the flanking peptides *in cellulo*. We thus follow the fibril formation and the cell viability induced by the peptides in the presence of a rat pancreatic β cell line (INS-1) or human islets. Both INS-1 cells and human islets were incubated in presence of 50 μM of N-terminal, C-terminal and a mixture of both peptide flanking peptides (ratio 1:1). No increase in ThT fluorescence intensity could be observed for the flanking peptides, suggesting that these peptides alone or together are not able to form fibrils in presence of INS-1 (Fig. 4C) nor in the presence of human islets (Fig. 4E), while the ThT signal increases after a few hours of incubation for mature hIAPP ($t_{1/2}$ of 5.5 ± 0.5 h in INS-1 cells and $t_{1/2}$ of 6.1 ± 0.5 h in human islets). To investigate the relationship between fibril formation and cell toxicity, we tested mature hIAPP and the flanking peptides on cell viability using both INS-1 cells and human islets (Fig. 4D-F, respectively). Cell viability was monitored by MTT assays for peptide samples at 50 μM. The non-fibrillogenic and nontoxic mouse IAPP

(mIAPP) peptide was used as a negative control. Mature hIAPP exhibits cytotoxicity with cell viability being reduced to 49 ± 5 % relative to the control cells after 24 h of incubation. In contrast, in the presence of the flanking peptides (alone or together with a ratio 1:1) at the same concentration, cell viability was not significantly affected as compared to the mIAPP and not reduced as compared to the mature hIAPP, with values from 79 to 95 %. We could measure a decrease in INS-1 cells viability when incubated in presence of C-terminal flanking peptide, which was not significative (Fig 4D). These results suggest that both flanking peptides are not fibrillogenic in model membranes neither in culture cells nor in human islets. The N-terminal flanking peptide is not toxic towards pancreatic cell lines neither towards human islets. Nevertheless, the C-terminal flanking peptide seems to have a slight toxicity towards INS-1 cells.

3.3. Do the flanking peptides influence mature hIAPP fibrillation in membrane models, in cells and in human islets?

The hIAPP precursor prohIAPP, that corresponds to the mature hIAPP covalently linked with the N- and C-terminal peptides, inhibit mature hIAPP fibril formation in the presence of membranes [37]. We next wanted to know if the flanking peptides could also interfere with mature hIAPP fibril formation and/or with hIAPP-induced membrane leakage when they are not covalently bound to the mature peptide but free in the media. Fig. 5A and 5B show respectively a time trace of dye leakage induced by the peptides and the calculated half-time ($t_{1/2}$) of hIAPP fibril formation and of hIAPP-induced membrane damage in the absence and in the presence of the flanking peptides. Our data indicate that the presence of the flanking peptides does not change the kinetics of membrane damage but decrease the extent of leakage from 62 % ± 5 % for hIAPP alone to 45 % ± 5 % for hIAPP and the C-terminal peptide and 39 % ± 5 % for hIAPP and the N-terminal peptide of the total vesicles content measured

after 16 h, suggesting that the flanking peptides somewhat reduce hIAPP-induced membrane damage. In addition, the kinetics of hIAPP fibril formation is slightly slowed down in the presence of the flanking peptides from 2.8 ± 0.6 h for hIAPP to 3.4 ± 0.8 h for hIAPP in the presence of the C-terminal peptide, 3.5 ± 0.6 h for hIAPP in the presence of the N-terminal peptide and 4.0 ± 0.6 h for hIAPP in the presence of both flanking peptides. These fluorescence data demonstrate that in the presence of membrane models the flanking peptides slightly decreased the kinetics of hIAPP fibril formation and the extent of hIAPP-membrane damage.

The composition of the β-cell granule is extremely complex. It is known that the C-peptide prevents insulin aggregation and that insulin inhibits hIAPP fibril formation [33,34, 56,57]. We next wanted to know whether the flanking peptides could interfere with mature hIAPP amyloidogenicity and toxicity in the presence of cultured cells and of human islets. INS-1 cells were incubated in presence of hIAPP alone or supplemented with the N-terminal, the C-terminal, or an equimolar mixture of N-terminal and C-terminal flanking peptides. The kinetics of fibril formation and the cell toxicity were determined for each condition. The time required to reach half-value of the maximum ThT signal ($t_{1/2}$) of mature hIAPP is in the same range as those for hIAPP in the presence of the flanking peptides, *i.e*, 5.9 ± 0.8 h for hIAPP alone and from 4.8 ± 0.8 h to 6.9 ± 0.8 h for hIAPP in the presence of the flanking peptides (Fig. 5C). The experiment in the presence of INS-1 cells reveals that the presence of the flanking peptides did not significantly affect the kinetics of hIAPP fibrillation (Fig. 5C). Mature hIAPP alone exhibits cytotoxicity with cell viability being reduced to 49 ± 5 % relative to the control cells after 24 h of incubation. In the presence of a flanking peptide, hIAPP presents the same cell toxicity (Fig. 5D) suggesting that the flanking peptides do not protect the cells from hIAPP toxicity.

The same experiments were then performed in human islets. In the presence of living human pancreatic islets, the transition from monomer to fibril formation occurs after 19.6 h ± 2.8 h (Fig. 5E). In the presence of the flanking peptide, this transition is slightly increased to 25.8 h ± 1.8 h with the N-terminal peptide and 24.7 h ± 2.0 h with the C-terminal peptide. In addition, the cell viability was determined and the results show that the toxicity is similar when human islets were incubated in presence of hIAPP alone or with the flanking peptides (Fig. 5F). Altogether our data suggest that hIAPP flanking peptides, produced during pro-hIAPP maturation, slightly alter hIAPP fibril formation but do not modify hIAPP toxic effect.

4. Discussions

Amyloid forming proteins are extremely sensitive to their environment therefore aggregation of amyloid proteins is easily influenced by both intrinsic and extrinsic factors. The relative importance of the flanking peptides and the possibility for interplay between mature hIAPP and the flanking peptides are the subject of the current investigation. In particular, we examine the potential alteration of mature hIAPP fibril formation, membrane damage and culture cells and human cells toxicity by the flanking peptides.

It has been showed that the C-peptide, issue from the maturation of the insulin, could promotes insulin disaggregation from its hexamer storage form, thus increasing insulin biological effect [39]. In contrary we demonstrated that the flanking peptides alone or together have a slight effect on hIAPP fibril formation but not on the resulting hIAPP-induced cell toxicity. Indeed, the flanking peptides slightly reduced hIAPP fibril formation and decreased the extent of membrane leakage. However, these peptides do not have any effect on hIAPP-induced cell death. Previous study proposed that the hIAPP precursors, proIAPP and proIAPP$_{1-48}$ which contain the mature hIAPP chemically linked to the flanking peptides,

prevent hIAPP aggregation and hIAPP-membrane damage *in vitro* [37]. This previous study combined with the current study demonstrates that the flanking peptides do have an important effect on hIAPP fibrillation when the flanking peptides are chemically covalently bound to mature hIAPP but not when they are free. These results suggest that the inhibition of hIAPP fibril formation by the proIAPP is not due to the particular amino-acids sequence of flanking peptides but rather to the conformation of flanking peptides covalently linked to the mature hIAPP.

The mechanism of hIAPP fibril formation was already described in solution and in the presence of artificial membranes and the hIAPP-induced cell toxicity was determined in cell lines [36,48,58–62]. However, it is interesting to connect the biophysical studies in models with the *in cellulo* experiments to provide a wealth of detailed mechanistic insights into the amyloid aggregation processes relevant to T2D. In this work, we studied hIAPP fibrillation in the presence of living cells and living human pancreatic islets to get insight into the mechanism of hIAPP fibrillation in living cells where the influence of biophysical properties (such as biomolecular solvation, viscosity, and excluded volume) and biochemical factors (such as the complex membrane systems and the presence of proteins) act in concert. We determined the time required to reach half-value ($t_{1/2}$) of the sigmoidal transition in the kinetics curves of ThT-fluorescence experiments in different media (solution, in negatively charged phospholipid membranes, in the presence of INS-1 cells or human islets). The $t_{1/2}$ varied from 2.8 h in the presence of phospholipid membranes to 19.6 h in the presence of pancreatic islets. This might be easily explained by the difference of buffer (phosphate buffer in the vesicles and cell culture media in the cells). However, our data show that the kinetics of fibril formation are faster in the cultured cells than in the media of the cultured cells suggesting that others biochemical factors such as the lipids and proteins present on the cell membranes inhibit mature hIAPP

fibril formation. Our study suggests that hIAPP flanking peptides are not an active contributor regulating the amyloidogenic propensity of hIAPP. Finally, since the C-peptide physiological activities have been ascribed on insulin target tissue, it is then tempting to propose that both flanking peptides, if they do not exert a clear activity on hIAPP fibrillation and toxicity, might nevertheless act on hIAPP target tissues.

5. Conclusions

Our results suggest that the flanking peptides are not amyloidogenic in solution, neither in the presence of phospholipid membranes or cultured cells. In solution and in the presence of phospholipidic model membranes, the flanking peptides slightly reduced hIAPP fibril formation and hIAPP-membrane damage. In the presence of human islets, the flanking peptides have somewhat tendency to reduce hIAPP fibril formation, while the hIAPP-induced cell toxicity is not affected.

Based on the results presented here and on our previous results [37], we conclude that the flanking peptides are important in inhibiting hIAPP fibril formation only when the peptides are covalently linked to the mature hIAPP but not free in solution. These data suggest that the particular amino-acids sequence of flanking peptides do not influence hIAPP fibrillation nor hIAPP-induced toxicity.

Acknowledgements

Christophe Piesse (Institut de Biologie Paris Seine, Sorbonne Université, France) is acknowledged for the peptides synthesis. We thank Ghislaine Frebourg (Institut de Biologie Paris Seine, Sorbonne Université, France) for her help in the electron microscopy experiments.

Corresponding Author

Lucie Khemtemourian

CNRS, UMR 7203 Laboratoire des Biomolécules, F-75005, Paris, France.

Tel: +33 1 44 27 61 83, E-mail address: lucie.khemtemourian@upmc.fr

Ghislaine Guillemain

INSERM, UMR_S938, Centre de recherche de St-Antoine, F- 75012 Paris, France

Tel: +33 1 40 01 13 54, E-mail address: ghislaine.guillemain@inserm.fr

Author Contributions

LK and GG designed the research; SSV, LK and GG performed experiments; PC and MA provided the human pancreatic islets; GG and LK interpreted data; GG and LK wrote the paper with input from BB. All the authors have approved the final article.

Funding

Sorbonne Université, CNRS, INSERM and the Saint-Antoine research center allowed this work to be performed.

6. Reference

[1] F. Chiti, C.M. Dobson, Protein Misfolding, Functional Amyloid, and Human Disease, Ann. Rev. Biochem. 75 (2006) 333–366.
[2] J.W.M. Höppener, B. Ahrén, C.J.M. Lips, Islet Amyloid and Type 2 Diabetes Mellitus, N. Engl. J. Med. 343 (2000) 411–419.
[3] P. Westermark, A. Andersson, G.T. Westermark, Islet Amyloid Polypeptide, Islet Amyloid, and Diabetes Mellitus, Physiol. Rev. 91 (2011) 795–826.
[4] E.L. Opie, The relation of diabetes mellitus to lesions of the pancreas. Hyaline degeneration of the islands of langerhans, J. Exp. Med. 5 (1901) 527–540.
[5] G.J. Cooper, A.C. Willis, A. Clark, R.C. Turner, R.B. Sim, K.B. Reid, Purification and characterization of a peptide from amyloid-rich pancreases of type 2 diabetic patients, Proc. Natl. Acad. Sci. U.S.A. 84 (1987) 8628–8632.
[6] P. Westermark, C. Wernstedt, E. Wilander, D.W. Hayden, T.D. O'Brien, K.H. Johnson, Amyloid fibrils in human insulinoma and islets of Langerhans of the diabetic cat are derived from a neuropeptide-like protein also present in normal islet cells, Proc. Natl. Acad. Sci. U.S.A. 84 (1987) 3881–3885.
[7] B. Gedulin, G.J.S. Cooper, A.A. Young, Amylin secretion from the perfused pancreas: Dissociation from insulin and abnormal elevation in insulin-resistant diabetic rats, Biochem. Biophys. Res. Commun. 180 (1991) 782–789.

[8] R.L. Hull, G.T. Westermark, P. Westermark, S.E. Kahn, Islet Amyloid: A Critical Entity in the Pathogenesis of Type 2 Diabetes, J. Clin. Endocrinol. Metab. 89 (2004) 3629–3643.
[9] S.E. Kahn, D.A. D'Alessio, M.W. Schwartz, W.Y. Fujimoto, J.W. Ensinck, G.J. Taborsky, D. Porte, Evidence of Cosecretion of Islet Amyloid Polypeptide and Insulin by -Cells, Diabetes. 39 (1990) 634–638.
[10] A. Lukinius, E. Wilander, G.T. Westermark, U. Engström, P. Westermark, Co-localization of islet amyloid polypeptide and insulin in the B cell secretory granules of the human pancreatic islets, Diabetologia. 32 (1989) 240–244.
[11] M. Stridsberg, S. Sandler, E. Wilander, Cosecretion of islet amyloid polypeptide (IAPP) and insulin from isolated rat pancreatic islets following stimulation or inhibition of beta-cell function, Regul. Pept. 45 (1993) 363–370.
[12] G. Blobel, Transfer of proteins across membranes. I. Presence of proteolytically processed and unprocessed nascent immunoglobulin light chains on membrane-bound ribosomes of murine myeloma, J. Cell Biol. 67 (1975) 835–851.
[13] T.A. Rapoport, Protein translocation across the eukaryotic endoplasmic reticulum and bacterial plasma membranes, Nature. 450 (2007) 663–669.
[14] R. Soong, J.R. Brender, P.M. Macdonald, A. Ramamoorthy, Association of Highly Compact Type II Diabetes Related Islet Amyloid Polypeptide Intermediate Species at Physiological Temperature Revealed by Diffusion NMR Spectroscopy, J. Am. Chem. Soc. 131 (2009) 7079–7085.
[15] P.J. Marek, V. Patsalo, D.F. Green, D.P. Raleigh, Ionic Strength Effects on Amyloid Formation by Amylin Are a Complicated Interplay among Debye Screening, Ion Selectivity, and Hofmeister Effects, Biochemistry. 51 (2012) 8478–8490.
[16] L. Khemtémourian, E. Doménech, J.P.F. Doux, M.C. Koorengevel, J.A. Killian, Low pH Acts as Inhibitor of Membrane Damage Induced by Human Islet Amyloid Polypeptide, J. Am. Chem. Soc. 133 (2011) 15598–15604.
[17] J.R. Brender, K. Hartman, R.P.R. Nanga, N. Popovych, R. de la Salud Bea, S. Vivekanandan, E.N.G. Marsh, A. Ramamoorthy, Role of Zinc in Human Islet Amyloid Polypeptide Aggregation, J. Am. Chem. Soc. 132 (2010) 8973–8983.
[18] S.J.C. Lee, T.S. Choi, J.W. Lee, H.J. Lee, D.-G. Mun, S. Akashi, S.-W. Lee, M.H. Lim, H.I. Kim, Structure and assembly mechanisms of toxic human islet amyloid polypeptide oligomers associated with copper, Chem. Sci. 7 (2016) 5398–5406.
[19] S. Salamekh, J.R. Brender, S.-J. Hyung, R.P.R. Nanga, S. Vivekanandan, B.T. Ruotolo, A. Ramamoorthy, A Two-Site Mechanism for the Inhibition of IAPP Amyloidogenesis by Zinc, J. Mol. Biol. 410 (2011) 294–306.
[20] J.D. Knight, A.D. Miranker, Phospholipid Catalysis of Diabetic Amyloid Assembly, J. Mol. Biol. 341 (2004) 1175–1187.
[21] J. Janson, R.H. Ashley, D. Harrison, S. McIntyre, P.C. Butler, The mechanism of islet amyloid polypeptide toxicity is membrane disruption by intermediate-sized toxic amyloid particles, Diabetes. 48 (1999) 491–498.
[22] E. Sparr, M.F.M. Engel, D.V. Sakharov, M. Sprong, J. Jacobs, B. de Kruijff, J.W.M. Höppener, J. Antoinette Killian, Islet amyloid polypeptide-induced membrane leakage involves uptake of lipids by forming amyloid fibers, FEBS Letters. 577 (2004) 117–120.
[23] T.A. Mirzabekov, M.C. Lin, B.L. Kagan, Pore formation by the cytotoxic islet amyloid peptide amylin, J. Biol. Chem. 271 (1996) 1988–1992.

[24] M. Anguiano, R.J. Nowak, P.T. Lansbury, Protofibrillar islet amyloid polypeptide permeabilizes synthetic vesicles by a pore-like mechanism that may be relevant to type II diabetes, Biochemistry. 41 (2002) 11338–11343.
[25] M. Gao, R. Winter, The Effects of Lipid Membranes, Crowding and Osmolytes on the Aggregation, and Fibrillation Propensity of Human IAPP, J. Diabetes Res. 2015 (2015) 1–21.
[26] M. Bongiovanni, F. Aprile, P. Sormanni, M. Vendruscolo, A Rationally Designed Hsp70 Variant Rescues the Aggregation-Associated Toxicity of Human IAPP in Cultured Pancreatic Islet β-Cells, Int. J. Mol. Sci. 19 (2018) 1443.
[27] B. Ward, K. Walker, C. Exley, Copper(II) inhibits the formation of amylin amyloid in vitro, Journal of Inorganic Biochemistry. 102 (2008) 371–375.
[28] Y.P. Yu, P. Lei, J. Hu, W.H. Wu, Y.F. Zhao, Y.M. Li. Copper-induced cytotoxicity: reactive oxygen species or islet amyloid polypeptide oligomer formation, Chem. Commun. 46 (2010) 6909-6911.
[29] A. Sinopoli, A. Magrì, D. Milardi, M. Pappalardo, P. Pucci, A. Flagiello, J.J. Titman, V.G. Nicoletti, G. Caruso, G. Pappalardo, G. Grasso, The role of copper(II) in the aggregation of human amylin, Metallomics. 10 (2014) 1841-1852.
[30] L. Ma, X. Li, Y. Wang, W. Zheng, T. Chen, Cu(II) inhibits hIAPP fibrillation and promotes hIAPP-induced beta cell apoptosis through induction of ROS-mediated mitochondrial dysfunction, J. Inorg. Biochem. 140 (2014) 143-52.
[31] S.J.C. Lee, T.S. Choi, J.W. Lee, H.J. Lee, D.G. Mun, S. Akashi, S.W. Lee, M.H. Lim, H.I. Kim, Structure and assembly mechanisms of toxic human islet amyloid polypeptide oligomers associated with copper, Chem. Sci. 8 (2016) 5398-5406.
[32] P. Westermark, Z.C. Li, G.T. Westermark, A. Leckström, D.F. Steiner, Effects of beta cell granule components on human islet amyloid polypeptide fibril formation, FEBS Lett. 379 (1996) 203–206.
[33] J.L. Larson, A.D. Miranker, The Mechanism of Insulin Action on Islet Amyloid Polypeptide Fiber Formation, J. Mol. Biol. 335 (2004) 221–231.
[34] E.T.A.S. Jaikaran, M.R. Nilsson, A. Clark, Pancreatic beta-cell granule peptides form heteromolecular complexes which inhibit islet amyloid polypeptide fibril formation, Biochem. J. 377 (2004) 709–716.
[35] A.C. Susa, C. Wu, S.L. Bernstein, N.F. Dupuis, H. Wang, D.P. Raleigh, J.E. Shea, M.T. Bowers, Defining the molecular basis of amyloid inhibitors: human islet amyloid polypeptide-insulin interactions, J. Am. Chem. Soc. 37 (2014) 12912-12919.
[36] L. Khemtemourian, G. Guillemain, F. Foufelle, J.A. Killian, Residue specific effects of human islet polypeptide amyloid on self-assembly and on cell toxicity, Biochimie. 142 (2017) 22–30.
[37] L. Khemtémourian, G. Lahoz Casarramona, D.P.L. Suylen, T.M. Hackeng, J.D. Meeldijk, B. de Kruijff, J.W.M. Höppener, J.A. Killian, Impaired Processing of Human Pro-Islet Amyloid Polypeptide Is Not a Causative Factor for Fibril Formation or Membrane Damage in Vitro, Biochemistry. 48 (2009) 10918–10925.
[38] G.L.C. Yosten, C. Maric-Bilkan, P. Luppi, J. Wahren, Physiological effects and therapeutic potential of proinsulin C-peptide, Am. J. Physiol. Endocrinol. Metab. 307 (2014) E955-968.
[39] J. Shafqat, E. Melles, K. Sigmundsson, B.-L. Johansson, K. Ekberg, G. Alvelius, M. Henriksson, J. Johansson, J. Wahren, H. Jörnvall, Proinsulin C-peptide elicits

disaggregation of insulin resulting in enhanced physiological insulin effects, Cell Mol. Life Sci. 63 (2006) 1805–1811.
[40] G. Rouser, S. Fkeischer, A. Yamamoto, Two dimensional then layer chromatographic separation of polar lipids and determination of phospholipids by phosphorus analysis of spots, Lipids. 5 (1970) 494–496.
[41] L.M. Green, J.L. Reade, C.F. Ware, Rapid colorimetric assay for cell viability: application to the quantitation of cytotoxic and growth inhibitory lymphokines, J. Immunol. Methods. 70 (1984) 257–268.
[42] O. Conchillo-Solé, N.S. de Groot, F.X. Avilés, J. Vendrell, X. Daura, S. Ventura, AGGRESCAN: a server for the prediction and evaluation of “hot spots” of aggregation in polypeptides, BMC Bioinformatics. 8 (2007) 65.
[43] S.O. Garbuzynskiy, M.Yu. Lobanov, O.V. Galzitskaya, FoldAmyloid: a method of prediction of amyloidogenic regions from protein sequence, Bioinformatics. 26 (2010) 326–332.
[44] A.-M. Fernandez-Escamilla, F. Rousseau, J. Schymkowitz, L. Serrano, Prediction of sequence-dependent and mutational effects on the aggregation of peptides and proteins, Nat. Biotechnol. 22 (2004) 1302–1306.
[45] M.J. Thompson, S.A. Sievers, J. Karanicolas, M.I. Ivanova, D. Baker, D. Eisenberg, The 3D profile method for identifying fibril-forming segments of proteins, Proc. Natl. Acad. Sci. U.S.A. 103 (2006) 4074–4078.
[46] S. Maurer-Stroh, M. Debulpaep, N. Kuemmerer, M.L. de la Paz, I.C. Martins, J. Reumers, K.L. Morris, A. Copland, L. Serpell, L. Serrano, J.W.H. Schymkowitz, F. Rousseau, Exploring the sequence determinants of amyloid structure using position-specific scoring matrices, Nat. Methods. 7 (2010) 237–242.
[47] H. LeVine, Quantification of beta-sheet amyloid fibril structures with thioflavin T, Meth. Enzymol. 309 (1999) 274–284.
[48] A.R.F. Hoffmann, L. Caillon, L.S. Salazar Vazquez, P.-A. Spath, L. Carlier, L. Khemtémourian, O. Lequin, Time dependence of NMR observables reveals salient differences in the accumulation of early aggregated species between human islet amyloid polypeptide and amyloid-β, Phys. Chem. Chem. Phys. 20 (2018) 9561–9573.
[49] C. Goldsbury, K. Goldie, J. Pellaud, J. Seelig, P. Frey, S.A. Müller, J. Kistler, G.J.S. Cooper, U. Aebi, Amyloid Fibril Formation from Full-Length and Fragments of Amylin, J. Struct Biol. 130 (2000) 352–362.
[50] L. Caillon, O. Lequin, L. Khemtémourian, Evaluation of membrane models and their composition for islet amyloid polypeptide-membrane aggregation, Biochim. Biophys. Acta. 1828 (2013) 2091–2098.
[51] M.F.M. Sciacca, C. Tempra, F. Scollo, D. Milardi, C. La Rosa. Amyloid growth and membrane damage: Current themes and emerging perspectives from theory and experiments on Aβ and hIAPP. Biochim. Biophys. Acta. 1860 (2018) 1625-1638.
[52] F. Scollo, C. Tempra, F. Lolicato, M.F.M. Sciacca, A. Raudino, D. Milardi, C. La Rosa. Phospholipids Critical Micellar Concentrations Trigger Different Mechanisms of Intrinsically Disordered Proteins Interaction with Model Membranes. J. Phys. Chem. Lett. 17 (2018) 5125-5129.
[53] X. Zhang, J.R. St Clair, E. London, D.P. Raleigh. Islet Amyloid Polypeptide Membrane Interactions: Effects of Membrane Composition. Biochemistry 56 (2017) 376-390.
[54] I. Rustenbeck, A. Matthies, S. Lenzen, Lipid composition of glucose-stimulated pancreatic islets and insulin-secreting tumor cells, Lipids. 29 (1994) 685–692.

[55] A.R.F. Hoffmann, M.S. Saravanan, O. Lequin, J.A. Killian, L. Khemtemourian, A single mutation on the human amyloid polypeptide modulates fibril growth and affects the mechanism of amyloid-induced membrane damage, Biochim. Biophys. Acta. 1860 (2018) 1783–1792.
[56] L. Wei, P. Jiang, Y.H. Yau, H. Summer, S.G. Shochat, Y. Mu, K. Pervushin, Residual Structure in Islet Amyloid Polypeptide Mediates Its Interactions with Soluble Insulin †, Biochemistry. 48 (2009) 2368–2376.
[57] W. Cui, J. Ma, P. Lei, W. Wu, Y. Yu, Y. Xiang, A. Tong, Y. Zhao, Y. Li, Insulin is a kinetic but not a thermodynamic inhibitor of amylin aggregation, FEBS Journal. 276 (2009) 3365–3371.
[58] P. Arosio, T.P.J. Knowles, S. Linse, On the lag phase in amyloid fibril formation, Phys. Chem. Chem. Phys. 17 (2015) 7606–7618.
[59] A. Chaari, M. Ladjimi, Human islet amyloid polypeptide (hIAPP) aggregation in type 2 diabetes: Correlation between intrinsic physicochemical properties of hIAPP aggregates and their cytotoxicity, Int. J. Biol. Macromol. 136 (2019) 57–65.
[60] J. Tan, J. Zhang, Y. Luo, S. Ye, Misfolding of a Human Islet Amyloid Polypeptide at the Lipid Membrane Populates through β-Sheet Conformers without Involving α-Helical Intermediates, J. Am. Chem. Soc. 141 (2019) 1941–1948.
[61] S. Asthana, B. Mallick, A.T. Alexandrescu, S. Jha, IAPP in type II diabetes: Basic research on structure, molecular interactions, and disease mechanisms suggests potential intervention strategies, Biochim. Biophys. Acta. 1860 (2018) 1765–1782.
[62] Y. Sun, A. Kakinen, Y. Xing, E.H. Pilkington, T.P. Davis, P.C. Ke, F. Ding, Nucleation of β-rich oligomers and β-barrels in the early aggregation of human islet amyloid polypeptide, Biochim. Biophys. Acta. 1865 (2019) 434–444.

Table 1. Comparison of the predicted amyloidogenicity of mature hIAPP and the two flanking peptides (N- and C-terminal) deduced by different amyloid prediction programs.

Name	Basic approach	Mature hIAPP	N-terminal	C-terminal
AGGREGASCAN	Composition of amino acids	5.77	0	0
FOLDAMYLOID	Composition of amino acids	Residue 13 to 18	0	Residue 12 to 16
TANGO	Properties of β-structural conformation	43.78	0	4.10
ZIPPERDB	Amyloid-like structures of short peptides	9	0	2
WALTZ	Amyloid-like structures of short peptides	Residue 22-29	Non amyloidogenic	Non amyloidogenic

Figure captions

Fig.1. Processing of human preproIAPP, through the secretory pathways in islet β cells, which leads to the formation of mature hIAPP and the two flanking peptides. The disulfide bridge is formed at the ER and the N-terminal signal peptide is cleaved after the transport to the *trans*-Golgi network. The cleavage of the C-terminus fragment (C: NAVEVLKREPLNYLPL) from prohIAPP is catalyzed by PC1/3. PC2 removes the N-terminal fragment (N: TPIESHQVEKR) of prohIAPP within the secretory vesicles. The remaining basic residues at the C-terminus are removed by the action of CPE. The final step of removal of Gly38 and amidation of hIAPP at the C-terminus is realized by the PAM complex.

Fig.2. (A) Kinetics of hIAPP fibril formation at different concentrations. The fluorescence curves were fitted to a Boltzmann equation to extract the maximal intensity at the plateau and half-time $t_{1/2}$. (B) Logarithmic plot of half-time $t_{1/2}$ *versus* hIAPP concentration. (C) Plot of the ThT fluorescence plateau intensity *versus* mature hIAPP (black circle) N-terminal peptide (grey square) and C-terminal peptide (white triangle) concentration.

Fig.3. Negatively stained microscopy images of mature hIAPP (A) after 24 h of incubation (scale bar 500 nm) and of the C-terminal (B) and N-terminal (C) flanking peptides after 4 days of incubation (scale bars 200 nm). Mature hIAPP (D) and flanking peptides (E-F) secondary structure changes followed by CD freshly dissolved (black), after 24 hours of incubation for hIAPP (grey) and after 48 h of incubation for the flanking peptides (grey).

Fig.4. (A) Kinetics of fibril formation (solid line with circles) and of membrane permeabilization (solid line) for mature hIAPP (blue) and the flanking peptides C-terminal

(purple) and N-terminal (green). (B) The average half-time ($t_{1/2}$) of the sigmoidal transitions for ThT fluorescence (dark grey) in the presence of DOPC/DOPS (7:3) LUVs and for membrane leakage (light grey) are shown for mature hIAPP and the flanking peptides alone and together. n.d. denotes the conditions at which the fit was not obtained due to the absence of aggregation. (C) Kinetics of mature hIAPP and the flanking peptides fibril formation at 50 µM in INS-1 β-cells. (D) Comparison of cell toxicity induced by mature hIAPP and the flanking peptides at a peptide concentration of 50 µM. Cell viability was measured after incubation of INS-1 β-cells with the peptide for 24 h using MTT assays. (E) Kinetics of mature hIAPP and the flanking peptides fibril formation at 50 µM in human islets. (F) Cell toxicity induced by mature hIAPP and the flanking peptides at a peptide concentration of 50 µM. Cell viability was measured after incubation of human islets with the peptide for 48 h using MTT assays.
Data represent mean ± SD of three replicate wells per condition (**p<0.01 and ****p<0.0001 compared to control condition).

Fig.5. Slight inhibition of hIAPP fibril formation and hIAPP-induced cell death induced by the flanking peptides. (A) Kinetics of membrane permabilization induced by 10 µM hIAPP alone (blue) and in the presence of one or two flanking peptides (purple: hIAPP+C-terminal peptide, green: hIAPP+N-terminal peptide and yellow: hIAPP+C- and N-terminal peptides). The peptides were added to the calcein-containing DOPC/DOPS (7:3) LUVs at time zero. (B) The average half-time ($t_{1/2}$) of the sigmoidal transitions for ThT fluorescence (dark grey) in the presence of DOPC/DOPS (7:3) LUVs and for membrane leakage (light grey) are shown for mature hIAPP in the presence of one flanking peptide (ratio hIAPP:flanking peptide 1:1) and in the presence of both flanking peptides (ratio 1:1). (C) Kinetics of mature hIAPP fibril formation in the presence of the flanking peptides (ratio 1:1) at 50 µM in INS-1 β-cells. (D) INS-

1 cell toxicity induced by mature hIAPP in the presence of the flanking peptides at a peptide concentration of 50 µM. (E) Kinetics of mature hIAPP fibril formation in the presence of the flanking peptides at 50 µM in human islets. (F) Human islets toxicity induced by mature hIAPP in the presence of the flanking peptides at a peptide concentration of 50 µM.

Data represent mean ± SD of three replicate wells per condition (*$p<0.05$, **$p<0.01$ and ****$p<0.0001$ compared to control condition).

Fig.1.

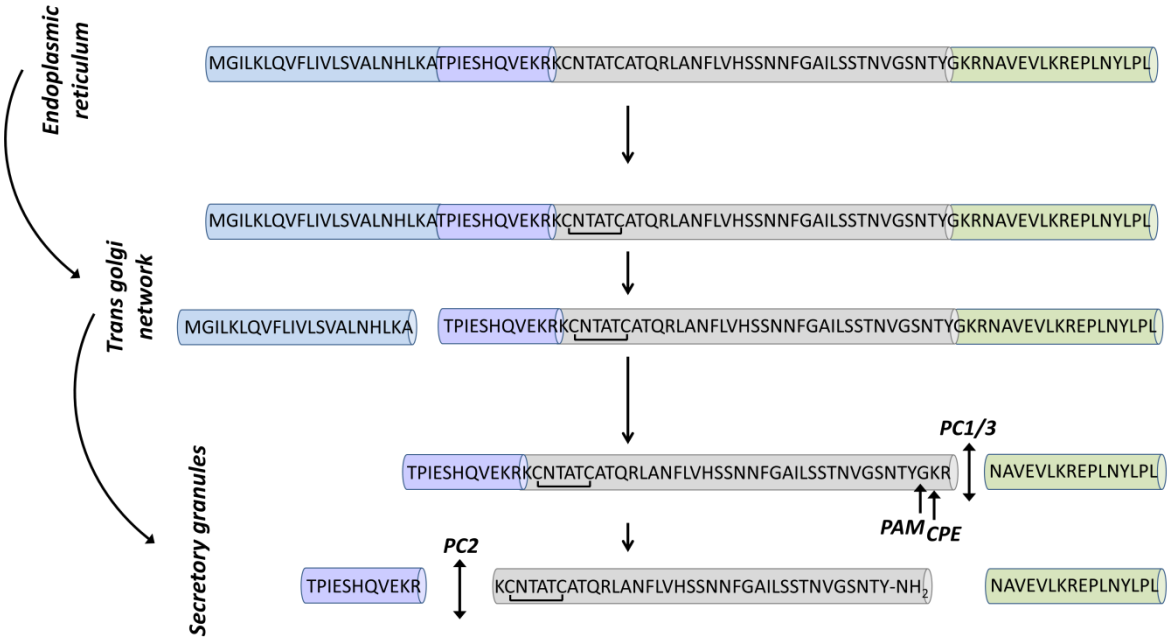
Endoplasmic reticulum
Trans golgi network
Secretory granules
MGILKLQVFLIVLSVALNHLKATPIESHQVEKRKCNTATCATQRLANFLVHSSNNFGAILSSTNVGSNTYGKRNAVEVLKREPLNYLPL
MGILKLQVFLIVLSVALNHLKA
TPIESHQVEKRKCNTATCATQRLANFLVHSSNNFGAILSSTNVGSNTYGKRNAVEVLKREPLNYLPL
PC1/3
PAM
CPE
PC2
TPIESHQVEKR
KCNTATCATQRLANFLVHSSNNFGAILSSTNVGSNTY-NH2
NAVEVLKREPLNYLPL

Fig.2.

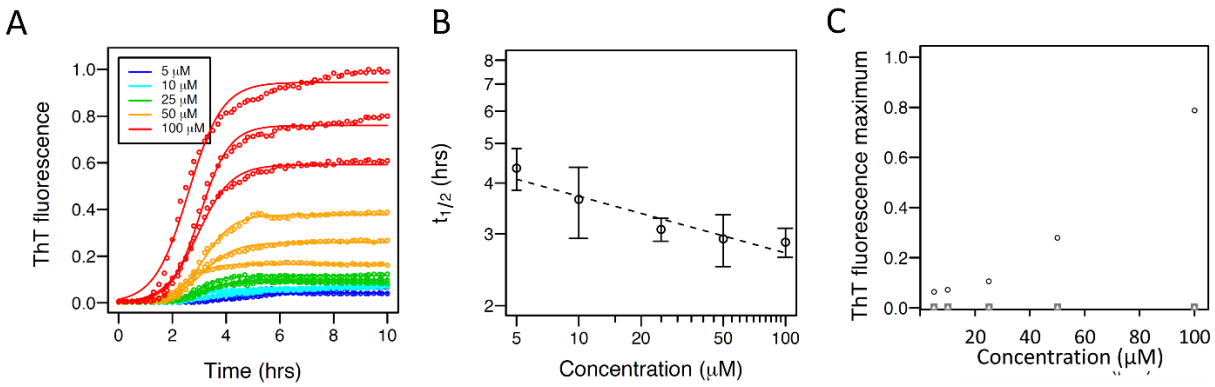
A
ThT fluorescence
Time (hrs)
5 μM
10 μM
25 μM
50 μM
100 μM
B
$t_{1/2}$ (hrs)
Concentration (μM)
C
ThT fluorescence maximum
Concentration (μM)

Fig.3.

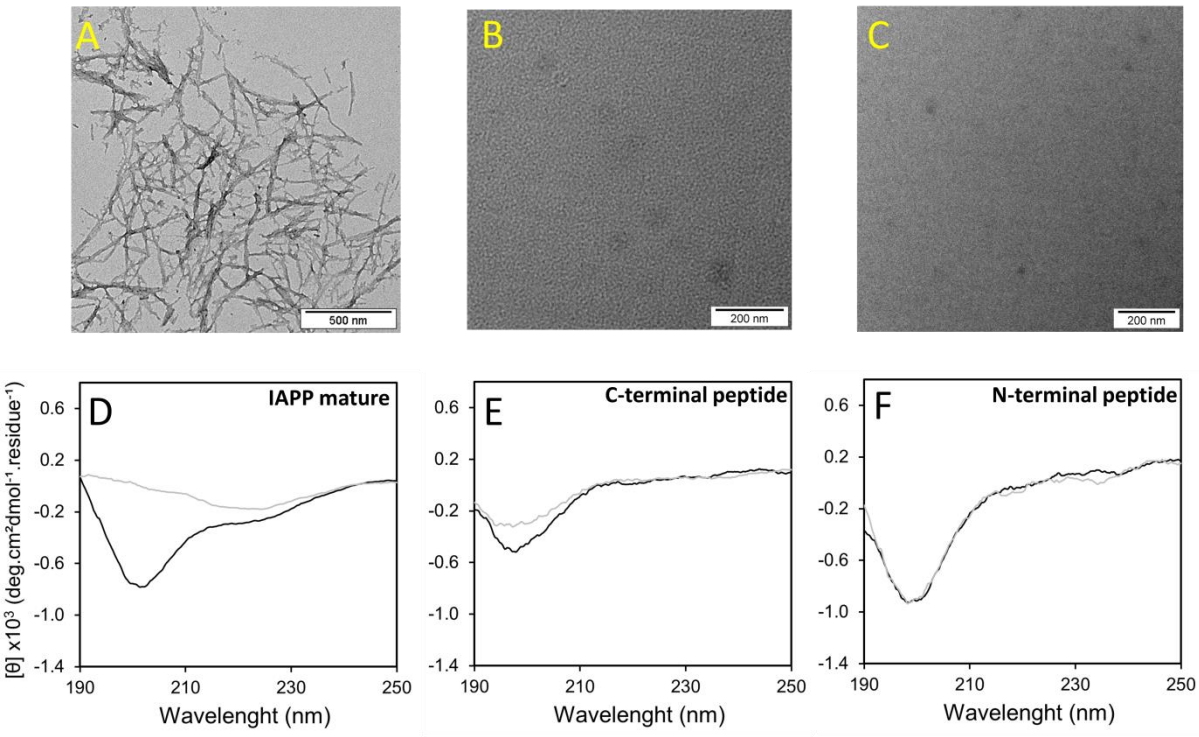
A
500 nm
B
200 nm
C
200 nm
D
IAPP mature
E
C-terminal peptide
F
N-terminal peptide
[θ] x10³ (deg.cm²dmol⁻¹.residue⁻¹)
0.6
0.2
-0.2
-0.6
-1.0
-1.4
190
210
230
250
Wavelenght (nm)

Fig.4.

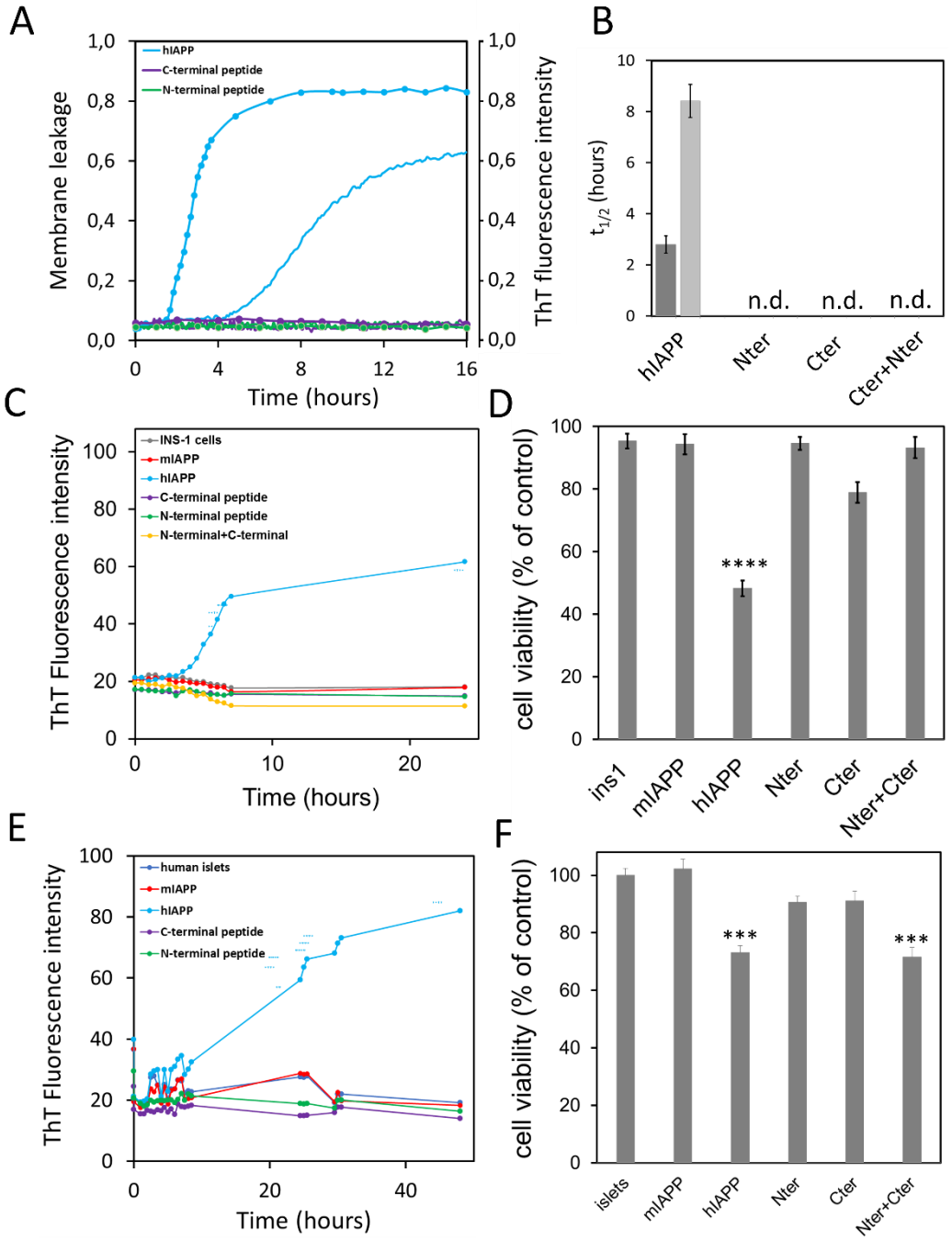
A
Membrane leakage
ThT fluorescence intensity
hIAPP
C-terminal peptide
N-terminal peptide
Time (hours)
B
t1/2 (hours)
n.d.
n.d.
n.d.
hIAPP
Nter
Cter
Cter+Nter
C
ThT Fluorescence intensity
INS-1 cells
mIAPP
hIAPP
C-terminal peptide
N-terminal peptide
N-terminal+C-terminal
Time (hours)
D
cell viability (% of control)
****
ins1
mIAPP
hIAPP
Nter
Cter
Nter+Cter
E
ThT Fluorescence intensity
human islets
mIAPP
hIAPP
C-terminal peptide
N-terminal peptide
Time (hours)
F
cell viability (% of control)
***
***
islets
mIAPP
hIAPP
Nter
Cter
Nter+Cter

Fig.5.

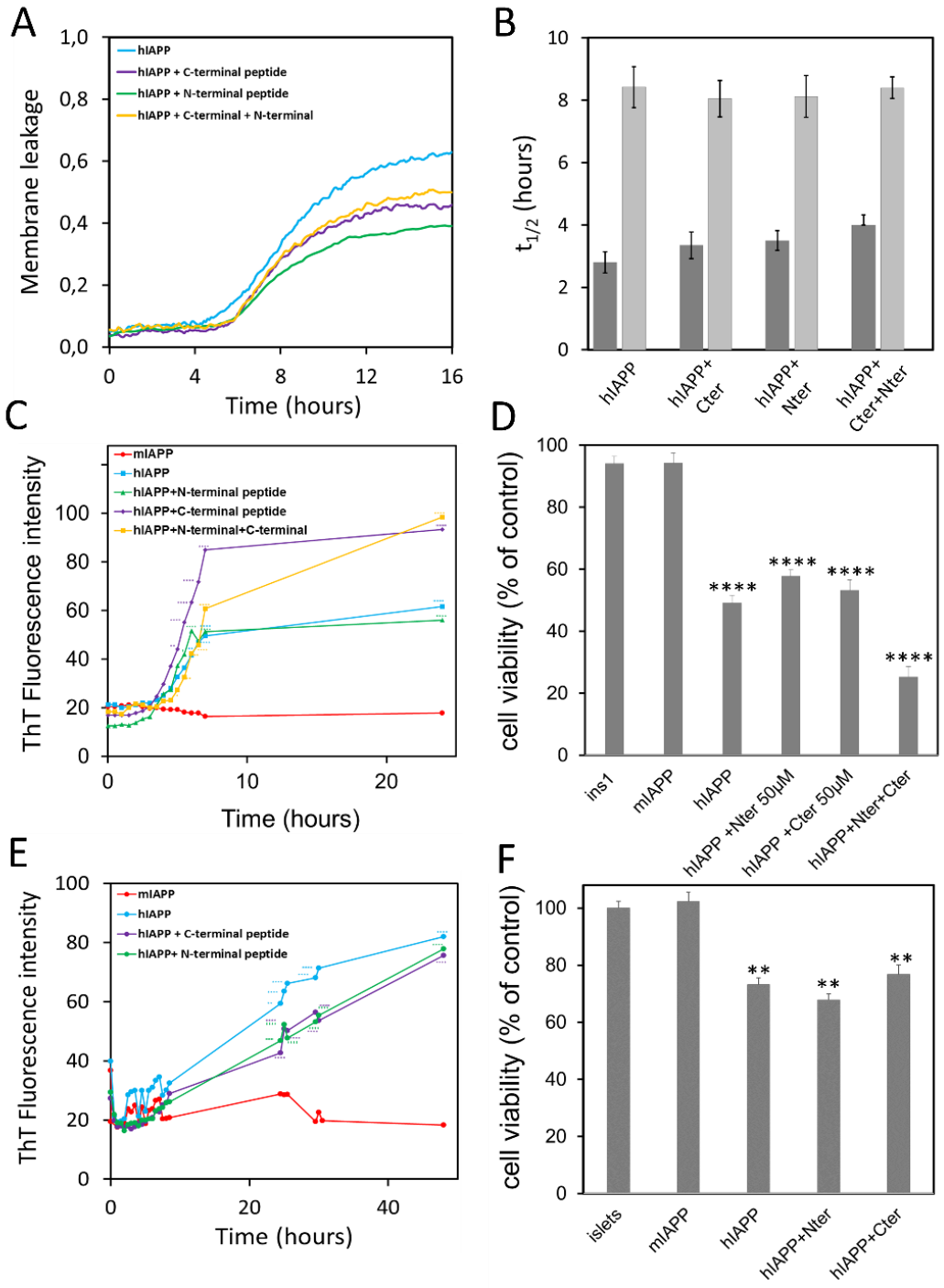
A
Membrane leakage
hIAPP
hIAPP + C-terminal peptide
hIAPP + N-terminal peptide
hIAPP + C-terminal + N-terminal
Time (hours)
B
t1/2 (hours)
hIAPP
hIAPP+ Cter
hIAPP+ Nter
hIAPP+ Cter+Nter
C
ThT Fluorescence intensity
mIAPP
hIAPP
hIAPP+N-terminal peptide
hIAPP+C-terminal peptide
hIAPP+N-terminal+C-terminal
Time (hours)
D
cell viability (% of control)
ins1
mIAPP
hIAPP
hIAPP +Nter 50µM
hIAPP +Cter 50µM
hIAPP+Nter+Cter
E
ThT Fluorescence intensity
mIAPP
hIAPP
hIAPP + C-terminal peptide
hIAPP+ N-terminal peptide
Time (hours)
F
cell viability (% of control)
islets
mIAPP
hIAPP
hIAPP+Nter
hIAPP+Cter